Modifying optical Bragg reflections from an antiferroelectric liquid crystal with photopolymer networks

Upindranath Singh and Shane Bradshaw
Physics Department, University of the West Indies, P.O. Box 64, Bridgetown, Barbados
(Received 8 January 2013; revised manuscript received 12 March 2013; published 30 April 2013)

By using an achiral monomer and a photoinitiator, we introduced polymer networks into the Sm-C^* phase of an antiferroelectric liquid crystal that forms ferro-, ferri-, and antiferroelectric phases. We then investigated the temperature dependence of Bragg wavelengths selectively reflected from these samples and found that the reflection bands shift to shorter wavelengths with increasing polymer concentration. The intermediate and the Sm-C^*_A phases dominate over the Sm-C^* phase for polymer concentration $\geqslant$4% by weight and the Sm-C^* phase disappears completely for a 6% polymer sample.

DOI: 10.1103/PhysRevE.87.042507 PACS number(s): 64.70.M−, 61.25.hp, 78.15.+e, 77.80.−e

I. INTRODUCTION

Apart from providing various challenges for the basic scientist, antiferroelectric liquid crystals (AFLCs) offer potential as display devices owing to their fast switching speeds [1]. The idea of developing materials that combine the mechanical strength of a polymer and the optical and electro-optical properties of a liquid crystal is quite attractive to display designers and manufacturers. If introduced into an antiferroelectric liquid crystal, polymer networks improve the alignment of the liquid crystal and reduce the switching times [2]. Photopolymerization, using either ultraviolet radiation or tuneable lasers, plays a central role in the preparation of blends for specific applications. Usually, a photoinitiator is required to introduce cross-linking within a liquid crystal-polymer blend [3]. However, some polymers contain photoreactive components that are sensitive to UV radiation and do not require a photoinitiator. Poly (vinyl cinnamate), for example, undergoes a random cross-linking photoaddition reaction when exposed to UV radiation.

Tilted chiral smectic liquid crystals are formed from rod-like molecules, which are aligned to form stacks of two-dimensional fluid-like layers. Within a given smectic layer, the molecules, on average, are tilted at a temperature-dependant angle θ with respect to the layer normal. The director (average orientation of the long molecular axes) of the ith smectic layer ($\mathbf{n}_i$) is defined by a tilt angle θ_i and an azimuthal orientation φ_i. The tilt angle is constant throughout the bulk sample and the layer to layer progression of φ_i distinguishes the various chiral smectic phases. The two main phases are the ferroelectric (Sm-C^*) and antiferroelectric (Sm-C^*_A) phases. Additional tilted thermodynamically stable phases have been identified (intermediate phases or subphases) and their structures combine both ferroelectric and antiferroelectric order. If all phases exist in an AFLC [4], the following phase sequence is observed: Iso↔Sm-A↔Sm-C^*_α↔Sm-C^*↔Sm-C^*_{FI2}↔Sm-C^*_{FI1}↔ Sm-C^*_A. Each phase has its own specific structure, which accounts for the significant differences in their optical, electrical, and electrooptical properties. However, if only nearest-neighbor interactions are present, none of the subphases has a lower free energy than that of the Sm-C^* or the Sm-C^*_A phase [5].

The preferential arrangement of tilted chiral smectics in a clock-like manner was first revealed by resonant x-ray scattering [6]. However, additional higher resolution x-ray resonant experiments [7,8], as well as optical rotation and ellipsometric data [9,10], strongly support a deformed clock model. The various phases are now classified according to their unit cell [11]. On this basis, the ferroelectric (Sm-C^*) phase consists of single, tilted, and polar smectic layers. The antiferroelectric (Sm-C^*_A) phase is characterized by a two-layer unit cell with opposite directions of the molecular tilt and two almost antiparallel electric dipoles. The Sm-C^*_{FI2} is a four-layered unit cell structure, while the Sm-C^*_{FI1} is three-layered. The Sm-C^*_α is an incommensurate structure with a helical period of the order of 6–7 smectic layers and, hence, has no well-defined unit cell.

The effects of doping on the phase stability and phases transitions in antiferroelectric liquid crystals have been reported by several groups. The dopants included carbon nanotubes [12], bent core molecules [2], chiral nonliquid crystalline dopants [7,13], chiral and nonchiral liquid crystalline materials [14], and opposite-handed enantiomers [15,16]. In general, these studies show that the stability of the antiferroelectric phase(s) is greatly enhanced in the doped materials. However, much less attention has been devoted to the steric effects of polymer networks on the corresponding phase transitions [2,17].

A chiral sematic liquid crystal with the appropriate macroscopic helical pitch selectively reflects visible light. This study seeks to explore the effects of polymer networks of varying cross-linking densities on the Bragg wavelengths selectively reflected by the various tilted phases. It has been found that if a network is formed while a sample is in a given liquid crystalline state, the thermodynamic range of stability of that phase is extended [18]. The hope is to stabilize the phases without disrupting their macroscopic helices, thus, enhancing their thermal and optical properties.

II. THEORY

The discrete clock model, which includes nearest-neighbor (NN), next-nearest-neighbor (NNN), and quadruple-NN interactions [4] accounts for all experimentally observed phases, including the intermediate Sm-C^*_{FI2} and Sm-C^*_{FI1} phases in AFLCs. This approach assumes that the free energy of the sematic system of N layers can be written as an expansion of

the structural (ξ) and polar (**P**) vector order parameters; ξ_i gives the magnitude and direction of the tilt in ith smectic layer while $\mathbf{P}_i$ represents the in-plane polarization and is perpendicular to ξ_i. The magnitude of ξ_i is the projection of the director ($\mathbf{n}_i$) onto the layer plane and it defines the tilt angle θ_i. The phase of the order parameter φ_i characterizes the azimuthal orientation of the tilt plane in the ith layer. Minimization of the free energy with respect to the polarization yields a relation between ξ and **P** [19–21].

Hence, the free energy may be written in terms of ξ only but with renormalized coefficients of expansion:

$$F_{\mathrm{Lan}} = \sum_i \left[\frac{1}{2}\alpha\,(T - T_c)\,\xi_j^2 + \frac{1}{4}b\xi_j^4\right], \qquad (1)$$

$$F_{\mathrm{int}} = \frac{1}{2}\sum_i \left[a_1\xi_i \cdot \xi_{i+1} + f(\xi_i \cdot \xi_{i+1})_z + a_2(\xi_i \cdot \xi_{i+1})^2\right]. \qquad (2)$$

Equation (1) represents the Landau terms where T_c is the transition temperature to the achiral Sm-A phase. The interlayer part of the free energy is given by Eq. (2). The first term in Eq. (2) is achiral and it describes the Van der Waals and polarization interactions between adjacent layers. A positive value of a_1 favors anticlinic ordering, whereas a negative coefficient favors synclinic ordering (ferroelectric and antiferroelectric order are roughly synclinic and anticlinic, respectively). The chiral term that leads to the formation of the microscopic helix is the second term in Eq. (2). The final term in Eq. (2) is the quadrupolar NN interaction energy, which represents a barrier energy [22] and accounts for the first-order antiferroelectric-ferroelectric transition. A numerical minimization [4,19–21,23] of the free energy over both the phase φ_i and the modulus θ_i of the order parameter ξ_i, for each i can account for the presence and stability of the intermediate phases as well as the fundamental phases.

III. MATERIALS AND EXPERIMENT

The antiferroelectric liquid crystal AS661 has also been referred to as 120F1M7 in the literature [24]. The material was purchased from Kingston Chemicals and used as received. The blends were prepared by mixing the desired amounts of the monomer 1-6-hexanediol-dimethacrylate (HDDMA), the photoiniatator Irgacure 651, and AS661. The blends were dissolved in a minimum amount of dry dichloromethane and dried at 60 °C in an inert atmosphere. The ratio of HDDMA and Irgacure 651 was kept fixed at 3:1 throughout. Samples of AS661 containing 1, 2, 3, 4, 5, and 6% by mass of the polymer-photoiniatator mixture were studied. The molecular structures of the materials used are shown in Fig. 1. For photopolymerization, we used an available 14-μW cm^{-2} UV source, which was calibrated to determine the optimum exposure time for complete photocrosslinking. Irradiation was performed while the samples were kept at a fixed temperature (corresponding to the midpoint of the Sm-C^* phase) on the hot stage of a Zeiss Axiolab Pol polarizing microscope, which was operating in the reflection mode. The change in the Bragg wavelengths reflected by a 1% doped sample with exposure times is shown in Fig. 2. The vertical line represents an exposure time of 20 min, which was chosen since the Bragg peaks are virtually time independent after this. This time was used for all subsequent experiments, even though higher concentrations of the photoiniatator will require less time for cross-linking.

Aqueous cetyl-trimethyl-ammonium bromide was used to prepare homeotropically aligned samples, which were

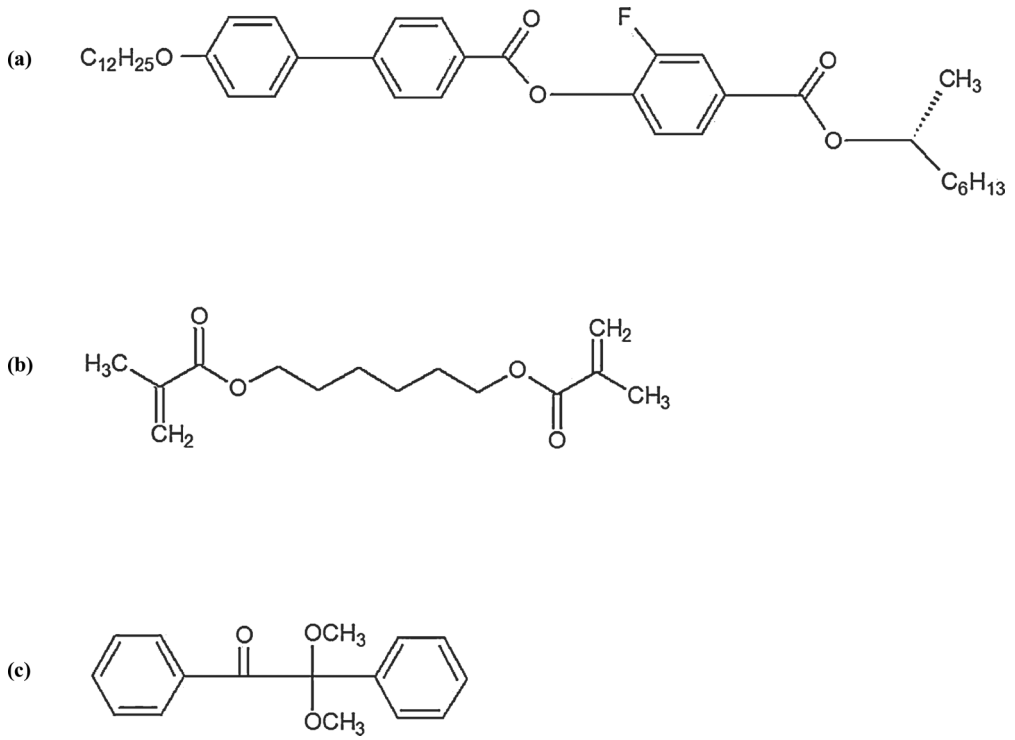

FIG. 1. Molecular structures of the material used: (a) AS661, (b) HDDMA, and (c) Irgacure 651.

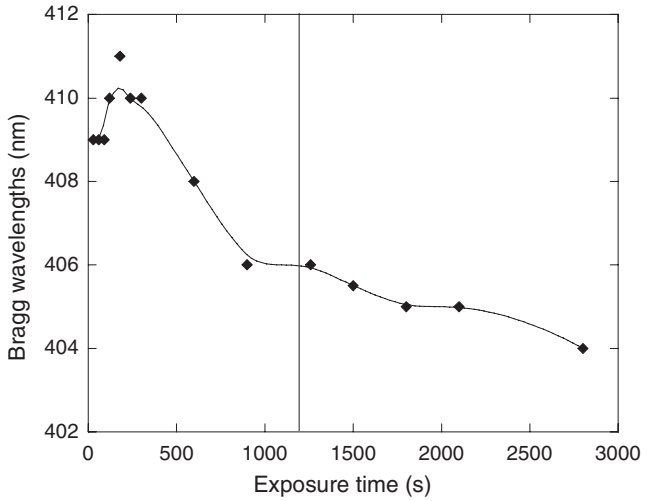

FIG. 2. Time dependence of Bragg selective reflections from a sample of AS661, which was doped with 1% polymer and then cross-linked. The UV light has an intensity of 14 μW cm^{-2}. The vertical line represents an exposure time of 20 m, which was used in all subsequent experiments.

contained between cover slips. The samples were heated into the isotropic phase, allowed to equilibrate (∼4 h), and then cooled at a rate of 1K h^{-1}. Temperature control to ± 0.005 K was achieved by using a combined HS1 heating stage and a MKI temperature controller (INSTEC). The Bragg detection system is shown in Fig. 3. The reflected light was diverted to a monochromator and then intercepted by a photomultiplier tube. Temperatures were kept fixed for 5 min before any readings were recorded. This time greatly exceeds that for data acquisition.

IV. RESULTS AND DISCUSSION

The textures of the various chiral smectic phases shown in Fig. 4 reveal that Bragg reflections in the visible region correspond to half-pitch and full-pitch reflections from the Sm-C^* phase and half-pitch reflections from the Sm-C^*_A phase [25]. The phase sequence and the corresponding transition temperatures of pure AS661 deduced from a combination of Bragg scattering data and direct observations with the polarizing microscope is:

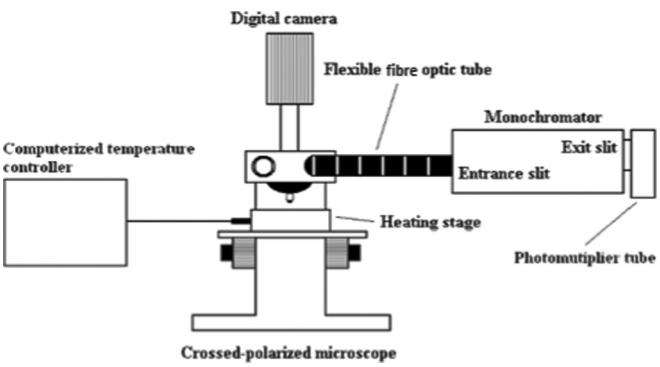

FIG. 3. Bragg scattering apparatus.

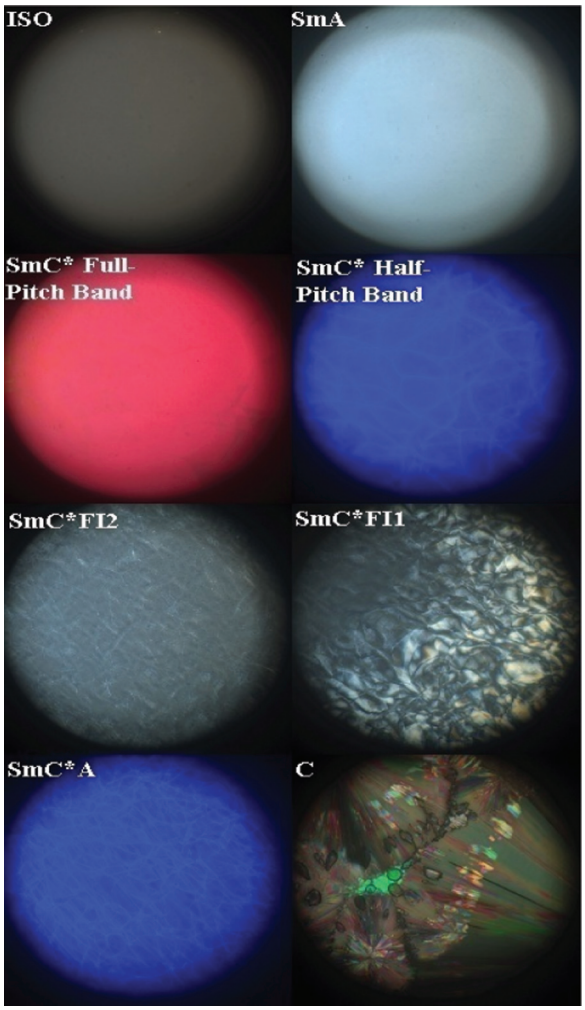

FIG. 4. (Color online) Color microscopic textures of the chiral smectic phases that appear in pure AS661 in the cooling mode (c refers to the crystalline phase). Images were viewed at x100 magnification.

Iso $\overrightarrow{106.75}$ Sm-A $\overrightarrow{91.55}$Sm-C^* $\overrightarrow{82.25}$Sm-C^*_{FI2} $\overrightarrow{78.95}$Sm-C^*_{FI1} $\overrightarrow{77.50}$ Sm-C^*_A $\overrightarrow{53.25}$ Cr

The Sm-C^*_α-Sm-A transition could not be identified from this experiment since both phases are nonreflecting and texture discrimination is not reliable.

The temperature dependence of the Bragg wavelengths selectively reflected from AS661 is shown in Fig. 5. The entire Sm-C^*_A range is visible, but both bands of the Sm-C^* phase are truncated at the upper and lower limits of our apparatus. The range of the Sm-C^* determined from the upper limit of the full-pitch reflections and the lower limit of the half-pitch reflection is 9.30 K. This range is consistent with previously published data [26]. Also, there is an interval of 0.80 K between the disappearance of the full-pitch reflections and the arrival of the half-pitch reflections for which Bragg peaks were not detected. Complete half-pitch and full-pitch bands (with the same topology) have been observed for a mixture of ferroelectric and antiferroelectric liquid crystals [27]. However, all these reflections are in the infrared region.

The pertinent features in Fig. 5 will be discussed before the data is analyzed. There is a region between the Sm-C^* and Sm-C^*_A phases that is devoid of Bragg reflections.

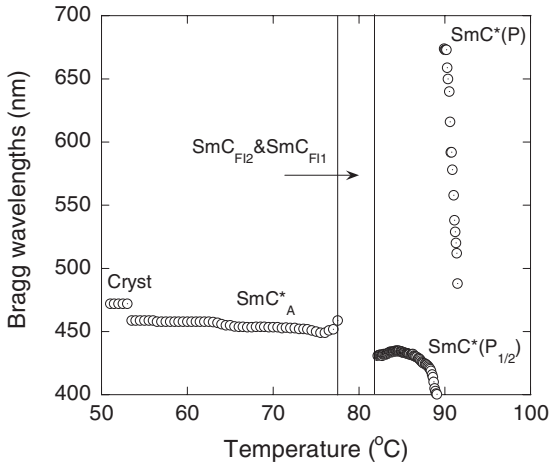

FIG. 5. Bragg wavelengths selectively reflected from AS661.

This region (4.75 K wide) corresponds to the Sm-C^*_{FI2} and Sm-C^*_{FI1} phases. If AS661 is cooled, full-pitch reflections first appear around 500 nm and change by ∼150 nm within a 1 °C temperature interval just below the transition to the Sm-C^* phase and then disappear. Hence, from Ref. [27], the initial half-pitch bands should appear around 250 nm and the maximum full-pitch bands around 860 nm (both wavelengths undetectable). Near the high-temperature end of the Sm-C^* phase, Bragg wavelengths increase rapidly with temperature but near the transition to the intermediate phases this dependence becomes quite weak. There is a broad but well-defined maximum around 435 nm in the half-pitch data. The corresponding Bragg wavelengths of the Sm-C^*_A phase is essentially constant over its entire temperature interval.

A prominent feature observed in chiral smectics is the anomalous temperature dependence of the helical pitch in the vicinity of the Sm-A-Sm-C^* phase transition [28–30]. The pitch has been observed to increase very rapidly just below the Sm-A-Sm-C^* transition (T_c), reach a maximum at ∼1 K below T_c, and then decrease slowly with decreasing temperature. Two similar generalized mean-field models which describe well the temperature dependence of the tilt angle, polarization, and their ratio have been developed [31,32]. However, these models give less desirable fits to the experimental pitch data, but the qualitative trends of the helical pitch anomaly are obtained.

In order to compare our results with theoretical predictions, we consider only the Landau terms of the free energy expression [31,32]. A minimization of the Landau free energy with respect to the wave vector (q) of the Sm-C^* phase yields the following expression:

$$q = \frac{2\pi}{p} = \frac{1}{\kappa_3}\left(\Lambda + \mu\frac{P}{\theta} + d\theta^2\right), \tag{3}$$

where κ_3 is a torsional elastic constant, Λ is the coefficient of the Lifshitz term, μ is a flexoelectric constant, P is the polarization, and d is a coupling coefficient. The anomalous temperature dependence of the helical pitch (p) has been attributed to competing contributions to q from the various terms of Eq. (3). Specifically, the P/θ term has to be of opposite sign to the first and third terms [33]. As the temperature is lowered below T_c, the wave vector (q) decreases (since P/θ increases), reaches a minimum, and then increases monotonically due to the higher-order (θ^2) term. Hence, the pitch ($p = 2\pi/q$) increases rapidly, assumes a maximum at ∼1 K below T_c, and then decreases at lower temperatures. An anomaly in the ratio of the polarization to the tilt angle (P/θ), which is closely related to the anomaly in the helical pitch, has also been observed.

We measured the temperature dependence of the Bragg wavelengths selectively reflected (λ_B), and in order to test the validity of the generalized mean-field model, Eq. (3) must be recast in a more appropriate form. Dumrongrattana *et al.* has found that neither the tilt nor the polarization could be fitted to a simple power of the form $\sim (T\text{-}T_c)^\beta$, with a single value β over any reasonable temperature interval [34]. The generalized mean free models [31,32] predict a crossover region where β changes value. In the region (T_c-T), ∼1 K the exponent β is mean field like ($\beta = 0.5$), and it decreases to $\beta = 0.25$ at lower temperatures. Hence, with this in mind we have replaced P/θ and θ in Eq. (3) by the simple temperature dependence $\sim(T\text{-}T_c)^\beta$ (P/θ and θ would have different temperature-dependent exponents). Since $d_B = \langle n\rangle\, p$, Eq. (3) may be rewritten as

$$\lambda_B = A + \frac{B}{(T_C - T)^\alpha} + \frac{C}{(T_C - T)^{2\beta}}, \tag{4}$$

where $A = \langle n\rangle\Lambda/2\pi k_3$, $B = \langle n\rangle\mu/2\pi k_3$, $C = \langle n\rangle d/2\pi k_3$, and α and β are exponents to be fitted. We have ignored the temperature dependence of average refractive index, since in a similar material it was found that the refractive indices both parallel and perpendicular to the director varied by <1% over the Sm-C^* range [35].

The temperature dependence of λ_B is captured in Fig. 6. The coefficients B and C are one order of magnitude greater

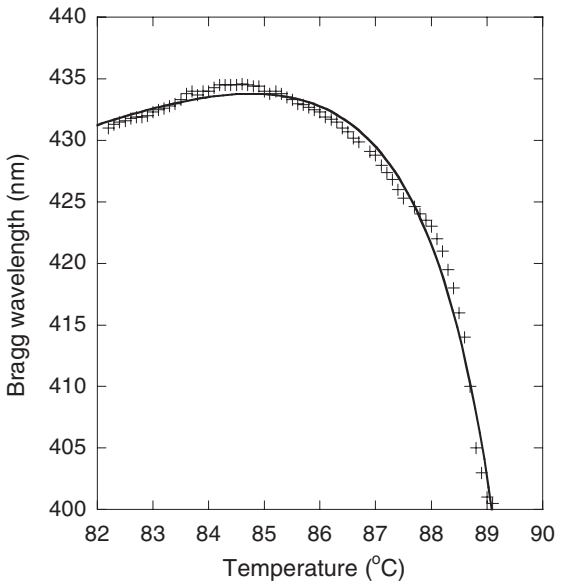

FIG. 6. Fitting the temperature dependence of d_B from the Sm-C^* phase to Eq. (4). The fitting parameters are: $A = 179.8 \pm 9.3$ nm; $B = 1160.5 \pm 38.2$ nm K$^{-\frac{1}{2}}$; $C = -1060.2 \pm 32.2$ nm K^{-1}. The exponents are $\alpha = 0.33 \pm 0.01$ and $\beta = 0.28 \pm 0.01$.

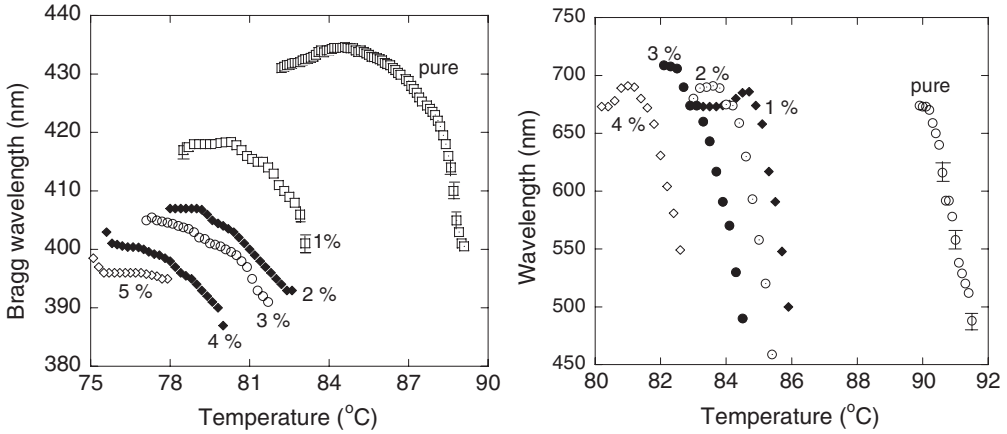

FIG. 7. The variation of half-pitch (left) and full-pitch (right) reflections with polymer concentrations for samples that were crossed linked in the Sm-C^* phase.

than A and are of opposite signs as expected. Although this fit is quite good, it only represents a portion of the Sm-C^* range. The highest temperature data begins at ~1.65 K below T_c, which is probably beyond the anomalous region since the exponents α and β (0.33 and 0.28, respectively) are both nonmean field. The values quoted for these exponents in the literature vary considerably [28,30,36–39]. This may be due to the temperature range of data used for fitting and/or the nature of the material.

Both half-pitch and full-pitch reflection bands were detected for samples that were cross-linked in the Sm-C^* phase. The temperature dependence of half-pitch and full-pitch reflections with polymer concentration is shown in Fig. 7. The entire Sm-C^* range can be easily deduced for all concentrations except the 5% case for which full-pitch reflections were absent. For half-pitch reflections, apart from the expected decrease in T_c, Bragg peaks are progressively shifted to shorter wavelengths and the temperature interval of stability decreases with increasing polymer concentration. This effect is opposite to what is normally observed if a chiral smectic is doped with a nonchiral molecule, since weakened chiral interactions would result in an increased pitch. However, strong anchoring of the molecules that are adjacent to the polymer strands prevents the liquid crystal molecule from adopting its normal equilibrium configuration. This nonequilibrium configuration has been confirmed by high-resolution x-ray diffraction. The introduction of a polymer network within the Sm-C^* phase of a chiral smectic liquid crystal decreases the effective tilt angle [40]. This has also been observed and illustrated by Archer, Dierking, and Osipov [41]. Our reflection data reveal that polymer networks can also generate a perturbed liquid crystalline state with a decreased pitch possibly by the distortion of a few smectic layers from within the helical structure.

The full-pitch bands are expected to have the same topology as half-pitch bands [27], but this is not quite obvious from Fig. 7, since data could only be measured over a temperature interval of ~1 K. The absence of full-pitch reflections from the 5% sample is more likely due to a distortion of the macroscopic helix by the polymer network created than by a shift of wavelengths to an undetectable region, since by extension these peaks should be around 600 nm and, hence, detectable. A further increase in polymer concentration to 6% resulted in a sample that was devoid of all Bragg reflections, which is consistent with the absence of any macroscopic helix.

The effect of polymer networks on the stability of the various phases is captured in Fig. 8. It is clear that the Sm-C^* is destabilized by the cross-linking in that phase, which is in direct contrast to results of Ref. [18]. The extrapolation of the data reveal that the Sm-C^* phase should disappear completely at a polymer concentration of 5.6%. Symonds, Davis, and Mitchell studied a nematic liquid crystal polymer whose kinetics owing to the additional effects of the polymer backbone and the absence of chiral interactions are expected to be vastly different from those of AFLCs. In fact, the FI1 and FI2 as well as the Sm-C^*_A phases are stabilized at the expense of the Sm-C^* phase. The network introduces an elastic contribution to the free energy of $\frac{1}{2}W_p\theta^2$ (W_p is an elastic coupling constant) [42]. It has been estimated that this elastic contribution to the free energy varies between 10 and 15% for a polymer network-stabilized ferroelectric

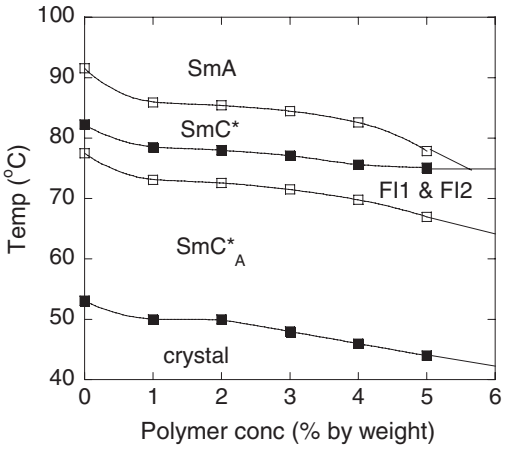

FIG. 8. Phase diagram showing the effect of polymer network concentration on the stability of the various chiral smectic phases of AS661.

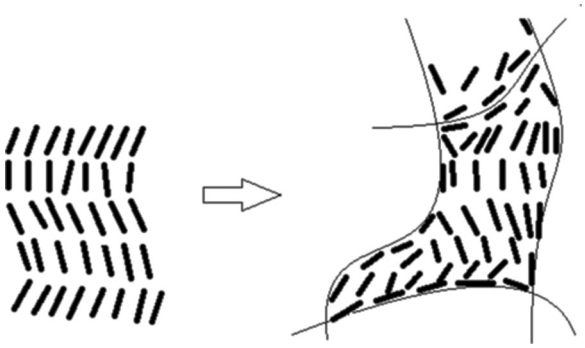

FIG. 9. Possible mechanism for the disruption of liquid crystalline order by the polymer networks created while the liquid crystal was in the Sm-C^* phase.

liquid crystal [41]. This elastic force is antagonistic toward liquid crystal alignment. Liquid crystal behavior is expected to dominate for low polymer concentrations. However, at higher polymer concentrations, strong anchoring of molecules that are adjacent to the polymer strands will prevent the liquid crystal from adopting its unperturbed configuration. Eventually, at concentrations $>5.6\%$ (extrapolated), the liquid crystal cannot form its macroscopic helix and, hence, the absence of Bragg reflections. The full-pitch reflections are expected to disappear first (as observed), since such bands require liquid crystalline order over the greater number of layers. This could also explain the stability of the FI1, FI2, and the Sm-C^*_A phases at the expense of the Sm-C^* phase. A possible mechanism for this destabilizing of the chiral Sm-C^* phase is shown in Fig. 9. The characterization of photopolymer networks formed in the Sm-C^* phase of ferroelectric liquid crystal has been reported in the literature [41]. The average polymer thickness was $\sim$130 nm and the order parameter was $\sim$0.9. Owing to the unavailability of a SEM, we were unable to perform similar measurements for our samples.

Since both doping and polymer networks stabilize the Sm-C^*_{FI2} Sm-C^*_{FI1} phases of AFLCs [2,7,13–17], we are able to determine which process is more effective by comparing the temperature intervals of the intermediate phases before and after irradiation with UV light. The results are contained in Fig. 10. Both doping and introducing polymer networks stabilize the intermediate phases, but doping is more effective. A possible explanation for this observation is that owing to the low polymer concentration, the dopant molecules are incorporated into the liquid crystal matrix and liquid crystalline order is preserved. Photocrosslinking occurs at a molecular level and the effect could be treated as a small perturbation. Hence, the network still provides a degree of stabilization despite being antagonistic toward liquid crystalline order.

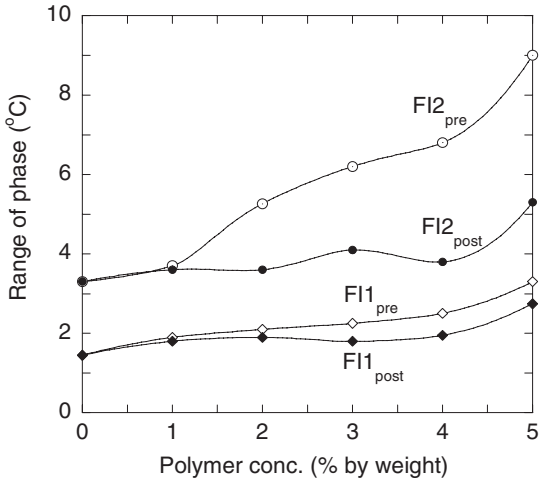

FIG. 10. The temperature intervals of the Sm-C^*_{FI2} and Sm-C^*_{FI1} phases before and after photopolymerization (pre and post). Each phase is plotted individually, and the lines are merely a guide to the eyes.

V. CONCLUSION

Antiferroelectric liquid crystals display both complex and intriguing phase behavior, and Bragg scattering is a sensitive and relative inexpensive technique for identifying transitions in such materials. The technique can identify all transitions except the Sm-C^*_α-Sm-A transition. This study explores the effect of polymer dopants on the phase sequence and phase stabilities of the chiral phases of AS661. Both full-pitch and half-pitch reflections (at least over a portion of the Sm-C^* phase) were detected even in the doped samples. For the pure material, since we could only detect half-pitch reflections starting at temperatures 1.65 K below T_c, we cannot comment on the anomalous region. The critical exponents P/θ and θ arising from the fitting of the temperature dependence of the Bragg wavelengths are 0.33 and 0.28, respectively, which represents nonmean field behavior.

It is clear from our results that polymer network stabilization opposes liquid crystalline order in the Sm-C^* phase of AFLCs. The intermediate and the Sm-C^*_A phases are stabilized at the expense of the Sm-C^* phase for polymer concentration $\geqslant 4\%$ by weight. In addition, both networks and doping stabilize the intermediate phases, but the dopant molecules provide a greater degree of stability than the photopolymer networks. If the polymer concentration is $<3\%$, the stability of Sm-C^* phase is not significantly affected, but the blends retain enough order to Bragg reflect visible light. With more prudent choice of photopolymers, it might be possible to combine both stability and desirable optical properties.

[1] S. T. Lagerwall, *Ferroelectric and Antiferroelectric Liquid Crystals* (Wiley-VCH, Weinheim, 1999).

[2] B. Atorf, A. Hoischen, M. B. Ros, N. Gimeno, C. Tschierske, G. Dantlgraber, and H. Kitzerow, Appl. Phys. Lett. **100**, 223301 (2012).

[3] C. V. Rajaram, S. D. Hudson, and L. C. Chien, Chem. Mater. **8**, 2451 (1996).

[4] M. Čepič, E. Gorecka, D. Pocienca, B. Žekš, and H. T. Nguyen, J. Chem. Phys. **117**, 1817 (2002).

[5] J. Prost and R. Bruinsma, Ferroelectrics **148**, 25 (1993).

[6] P. Mach, R. Pindak, A. M. Levelut, P. Barois, H. T. Nguyen, C. C. Huang, and L. Furenlid, Phys. Rev. Lett. **81**, 1015 (1998).
[7] N. W. Roberts, S. Jaradat, L. S. Hirst, M. S. Thurlow, Y. Wang, S. T. Wang, Z. Q. Liu, C. C. Wang, J. Bai, H. Pindak, and H. F. Gleeson, Europhys. Lett. **72**, 976 (2005).
[8] A. Cady, J. A. Pitney, R. Pindak, L. S. Matkin, S. J. Watson, H. F. Gleeson, P. Cluzeau, P. Barois, A.-M. Levelut, W. Caliebe, J. W. Goodby, M. Hird, and C. C. Huang, Phys. Rev. E **64**, 050702 (2001).
[9] I. Muševič and M. Škarabot, Phys. Rev. E **64**, 051706 (2001).
[10] P. M. Johnson, D. A. Olson, S. Pankratz, T. Nguyen, J. Goodby, M. Hird, and C. C. Huang, Phys. Rev. Lett. **84**, 4870 (2000).
[11] I. Muševič, R. Blinc, B. Žekš, M. Čopič, M. M. Wittebrood, T. Rasing, H. Orihara, and Y. Ishibashi, Phys. Rev. Lett. **71**, 1180 (1993).
[12] Jan P. F. Lagerwall, R. Dabrowski, and G. Scalia, J. Non-Cryst. Solids **353**, 4411 (2007).
[13] S. Jaradat, N. W. Roberts, Y. Wang, L. S. Hirst, and H. F. Gleeson, J. Mater. Chem. **16**, 3753 (2006)
[14] J. Kirchhoff and L. S. Hirst, Phys. Rev. E **76**, 051704 (2007).
[15] E. Gorecka, D. Pociecha, M. Čepič, B. Žekš, and R. Dabrowski, Phys. Rev. E **65**, 061703 (2002).
[16] A. Cady, Z. Q. Liu, X. F. Han, S. T. Wang, M. Veum, N. Janarthanan, C. S. Hsu, D. A. Olson, and C. C. Huang, Phys. Rev. E **66**, 061704 (2002).
[17] U. Singh and H. F. Gleeson, Ferroelectrics **321**, 53 (2005).
[18] A. Symons, F. J. Davis, and G. R. Mitchell, Liquid Crystallogr. **14**, 853 (1993).
[19] M. Čepič and B. Žekš, Phys. Rev. Lett. **87**, 085501 (2001).
[20] M. Conradi, I. Muševič, and M. Čepič, Phys. Rev. E **65**, 061705 (2002).
[21] N. Vaupotič and M. Čepič, Phys. Rev. E **71**, 041701 (2005).
[22] H. Orihara and Y. Ishibashi, Jpn. J. Appl. Phys., Part 2 **29**, L115 (1990).
[23] P. V. Dolganov, V. M. Zhilin, V. K. Dolganov, and E. I. Kats, Phys. Rev. E **67**, 041716 (2003).
[24] V. P. Panov, N. M. Shtykov, A. Fukuda, J. K. Vij, Y. Suzuki, R. A. Lewis, M. Hird, and J. W. Goodby, Phys. Rev. E **69**, 060701 (2004).
[25] R. B. Meyer, L. Libert, L. Strzelecki, and P. Keller, J. Phys. (Paris), Lett. **36**, L69 (1975).
[26] V. P. Panov, J. K. Vij, Yu. P. Panarin, C. Blanc, V. Lorman, and J. W. Goodby, Phys. Rev. E **75**, 042701 (2007).
[27] K. L. Sandhya, A. D. L. Chandani-Perera, A. Fukuda, J. K. Vij, and K. Ishikawa, Europhys. Lett. **19**, 56005 (2010).
[28] A. Seppen, I. Muševič, G. Maret, B. Žekš, P. Wydner, and R. Blinc, J. Phys. (France) **49**, 1569 (1988).
[29] B. I. Ostrovskiĭ, A. Z. Rabinovich, A. S. Sonin, and B. A. Strukov, Zh. Eksp. Teor. Fiz **74**, 1748 (1978).
[30] S. A. Pikin and V. L. Indenbom, Sov. Phys. Usp. **21**, 487 (1978).
[31] C. C. Huang and S. Dumrongrattana, Phys. Rev. A **34**, 5020 (1986).
[32] B. Žekš, Mol. Cryst Liquid Crystallogr. **114**, 259 (1984).
[33] B. Kutnjak-Urbanc and B. Žekš, Phys. Rev. E **51**, 1569 (1995).
[34] S. Dumrongrattana, C. C. Huang, G. Nounesis, S. C. Lien, and J. M. Viner, Phys. Rev. A **34**, 5010 (1986).
[35] N. W. Roberts, H. F. Gleeson, N. Bowring, A. Seed, L. N. Nassif, M. R. Herbert, J. W. Goodby, and M. Hird, J. Mater. Chem. **13**, 353 (2003).
[36] H. Uehara, T. Yata, and J. Hatano, J. Korean Phys. Soc. **32**, S1063 (1998).
[37] I. Abdulhalim, L. Benguigui, and R. Weil, J. Phys. (France) **46**, 1429 (1985).
[38] B. I. Ostrovskiĭ, A. Z. Rabinovich, A. S. Sonin, B. A. Strukov, and N. I. Chernova, Zh. Eksp. Teor. Fiz **25**, 80 (1977).
[39] S. S. Bhattacharyya, A. Mukherjee, B. K. Chaudhuri, and S. L. Wu, Indian J. Pure Appl. Phys. **47**, 372 (2009).
[40] U. Singh, Phys. Rev. E **83**, 061707 (2011).
[41] P. Archer, I. Dierking, and M. Osipov, Phys. Rev. E **78**, 051703 (2008).
[42] M. Brehmer, R. Zentel, F. Giesselmann, R. Germer, and P. Zugenmaier, Liquid Crystallogr. **21**, 589 (1996).